Energy Materials 2014
The Chinese Society for Metals (CSM) and The Minerals, Metals & Materials Society (TMS)
TMS, 2014

CREEP STRENGTH BEHAVIOR OF BORON ADDED P91 STEEL AND ITS WELD IN THE TEMPERATURE RANGE OF 600–650°C

J.Swaminathan[1] C.R. Das[2] Jayashree Baral[3], C. Phaniraj[2] R.N. Ghosh[3]
S.K. Albert[2], and A.K.Bhaduri[2],

[1]National Metallurgical Laboratory, Jamshedpur -831007,INDIA
[2]Indira Gandhi Centre for Atomic Research, Kalpakkam -603102 INDIA
[3]Indian Institute of Technology, Kharagpur-721302,India

Keywords: Type IV cracking, P91 steel, Boron addition, creep

Abstract

One of the promising ways for mitigation of Type IV cracking – a failure by cracking at the intercritical /fine grained heat affected zone, a life limiting problem in advanced 9–12 Cr ferritic steel weld like that of P91 is through modification of alloy composition by addition of boron. Addition of boron was observed to improve the microstructure at the weld zone and hence the creep strength. In the present work, boron (100 ppm with controlled nitrogen) added P91 steel after normalizing at 1050°C and 1150°C and tempered at 760°C were studied for the creep behavior in the base metal and welded condition in the temperature range of 600–650°C. Creep strength was characterized in terms of stress and temperature dependence of creep rate and rupture time. Weld creep life was reduced compared to the base metal with rupture occurring at the ICHAZ (Type IV crack). However at longer time (at lower stress levels) exposure creep crack moves from weld metal to HAZ (Type II crack). Rupture life was found to superior for the base and weld in the boron containing steel when higher normalizing temperature is used. Estimation of 10^5 h was attempted based on short term rupture data available and weld strength factors were calculated. Observed values are better for P91BH condition than the values for P91BLcondition as well as those available for P91 in open literature

Introduction

The advent of ultra super critical plants has resulted in development of 9–12% Cr ferritic–martensitic steels with better resistance to high temperature creep and corrosion in addition to thermal conductivity and lower cost than austenitic stainless steels [1–3]. Modified 9Cr–1Mo (P91) steel derives higher creep strength from the presence of stable carbides and carbo-nitrides which provide resistance to motion of free dislocations [3]. However, premature failures of weldments have been reported [4] in the intercritical/ fine grain regions of heat affected zone (HAZ) which is popularly known as Type IV cracking, and has been commonly attributed to the lower creep strength of these regions when compared to base metal. There are studies that show [5–7] that the addition of boron improves resistance to creep and type IV cracking in ferritic steels. The observed beneficial effect was attributed [6] to the microstructural changes like uniform prior austenitic grain size in HAZ and stabilization of precipitates which delays the substructure development.

Das and co–workers [8–11] have observed that 100 ppm boron containing P91 steel (P91B) exhibited lower minimum creep rates and enhanced creep–rupture lives compared to boron free P91 steel at 600–650°C for normalized (1050°C/1h) and tempered (760°C/3h) condition. The

effect of different normalizing temperatures on creep properties was also investigated [8–11] and it was observed that unlike P91 steel, the P91B steel showed improved creep strength at higher normalizing temperature of 1150°C/1h compared to 1050°C/1h. In this paper, 1150°C/1h is designated as P91BH whereas 1050°C/1h is referred to as P91BL. Encouraged by the beneficial effect of higher normalizing temperature for P91B steel, a systematic study has been carried out to characterize the creep behavior of P91BL and P91BH for base and weldments at creep test temperatures of 600, 625 and 650°C. This paper discusses the results of creep tests along with microstructural analysis

2. EXPERIMENTAL PROCEDURE

2.1 Material

The material used in this study is modified 9Cr–1Mo steel containing 100 ppm boron and 20 ppm nitrogen and the steel was melted in vacuum induction furnace followed by vacuum arc re-melting. Hot rolled plates were tempered at 760°C/3h. Two types of heat treatment (differing in normalizing temperature) were given to the as-received plates. One was normalizing at 1050°C/1h (i.e., P91BL) and another at 1150°C/1h (i.e., P91BH) followed by air cooling. All the plates were tempered at 760°C/3h and cooled in furnace. The weld joints were fabricated from these plates.

The chemical composition of P91B steel is listed in Table 1. Nitrogen level in this steel was deliberately lowered to avoid formation of boron nitride as boron has a strong affinity for nitrogen. Manual metal arc welding (MMAW) process was used for welding. Due to non-availability of boron containing P91 welding consumable, modified P91 steel electrodes were used. Preheating and inter–pass temperature of 200–250°C was maintained during the welding. Welding parameters employed are given in Table 2. To improve ductility, reduce residual stress and to increase thermal stability of microstructure the weldments were subjected to post weld heat treatment (PWHT) at 760°C for 3h.

Table 1 Chemical composition of P91B steel (in Wt. %)

C	Si	Mn	P	S	Cr	Mo	V	Nb	Ni
0.10	0.40	0.30	0.005	0.002	8.50	1.04	0.090	0.10	0.020
Al	N	B	Fe						
0.030	0.0021	0.010	Bal.						

Table 2. Welding parameters used for P91B steel weld joints

Welding method	Current (A)	Voltage (V)	Heat input (kJ/mm)
MMAW	100	25	1.0

2.2 Microstructural Characterization

Microstructure was examined using optical and electron microscope (SEM, TEM). Optical microscopic specimens were etched with Villella"s reagent (1g Picric acid + 5ml HCl + 100ml methanol).

2.3 Creep test

Constant load creep tests were performed on MAYES machine (Model TC 30). Cylindrical creep test specimens with 6 mm in diameter over 50 mm gauge length were machined from the base

and weld joints of 12 mm thick plate of P91B steel. Specimens were fabricated in such a way that the weld metal was located in the center of specimen. The strain was measured by an extensometer–LVDT assembly. Creep tests were conducted on base metal and weld joints for both P91BL and P91BH in the stress range of 210-70 MPa at temperatures 600, 625 and 650°C. The test temperature was controlled with an accuracy of ±2°C

3. RESULTS

3.1. Microstructure and hardness

Microstructure of P91BL and P91BH base metals are shown in **Fig.1 (a,b)**. It is observed that the prior austenite grain boundaries as well as packet, block and lath boundaries are decorated with precipitates, formed during tempering. It also shows that the precipitates are aligned along the lath boundaries, in addition to packet and prior austenite grain boundaries

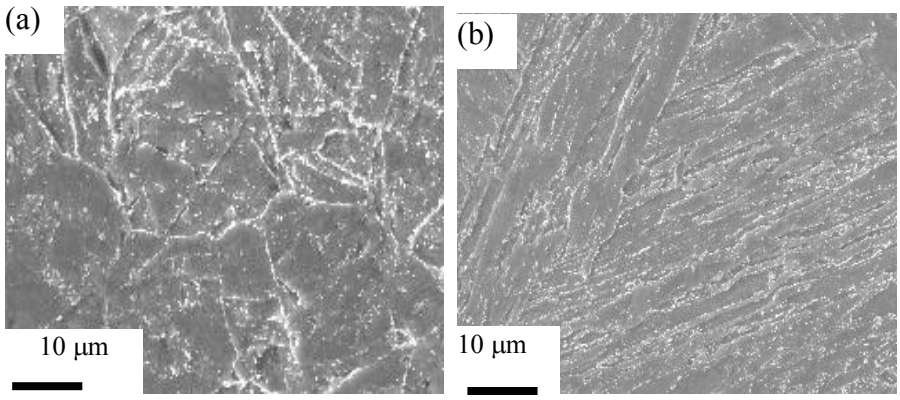

Figure. 1 Secondary electron image of N&T P91B steel: (a) P91BL (1050°C) and (b) P91BH (1150°C).

The frequency distribution plots of precipitate sizes, measured from the secondary electron images for P91BL and P91BH are shown in Figures.2 (a) and (b)**,** respectively. Higher fraction of fine precipitates in P91BH than in P91BL is apparent from Figure.2. Though, $M_{23}C_6$ precipitates are larger compared to MX type, it may be mentioned that the frequency distribution plot as shown in Figure.2 is obtained without considering the type of precipitate. This is because; it is difficult in SEM to identify the precipitate. Precipitates below 40 nm were not considered for estimating the size. It is well known that MX type precipitates are stable and provide high temperature creep strength in P91 steel

3.2 Creep behavior

Typical creep curves for P91BL and P91BH are shown in Figure.3 (a) and (b)**,** respectively for different test temperatures for both base and weldments. Whereas, creep rate vs. time plots for base and weldments at low and high temperature normalizing conditions are shown in Figure.3 (c) and (d). For base and weldment, at all test temperatures and stresses, creep curves of P9BL and P91BH showed a brief normal transient creep regime followed by minimum creep rate and tertiary creep region leading to failure. Distinct steady–state creep region was not observed. At all test conditions, creep ductility was found to decrease with decrease in stress.

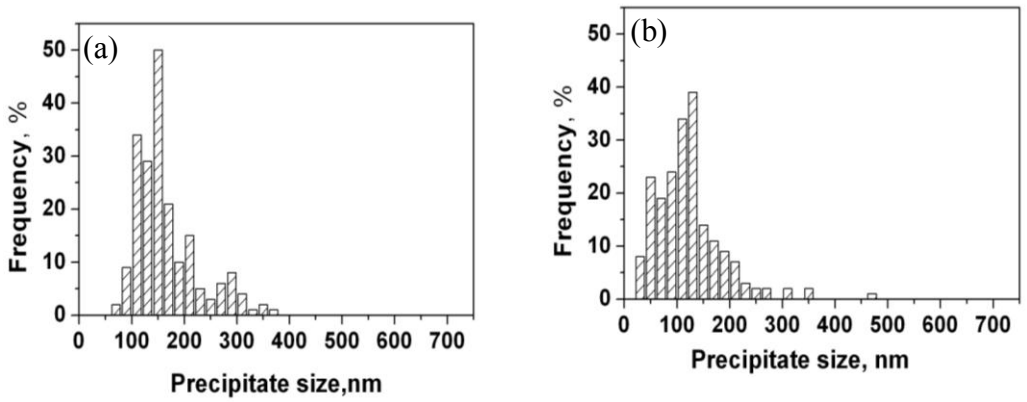

Figure. 2 Frequency distribution of precipitate size in (a) P91BL and (b) P91BH steels

For the base metal, Figures 4a and 4b shows the stress dependence of minimum creep rate for base metal and cross weld specimens of P91BL and P91BH at test temperatures. For P91BL and P91BH, the variation of creep–rupture life with stress is shown in Figures 5a and 5b for the base metal and for cross weld specimens at test temperatures for both P91BL and P91BH conditions.

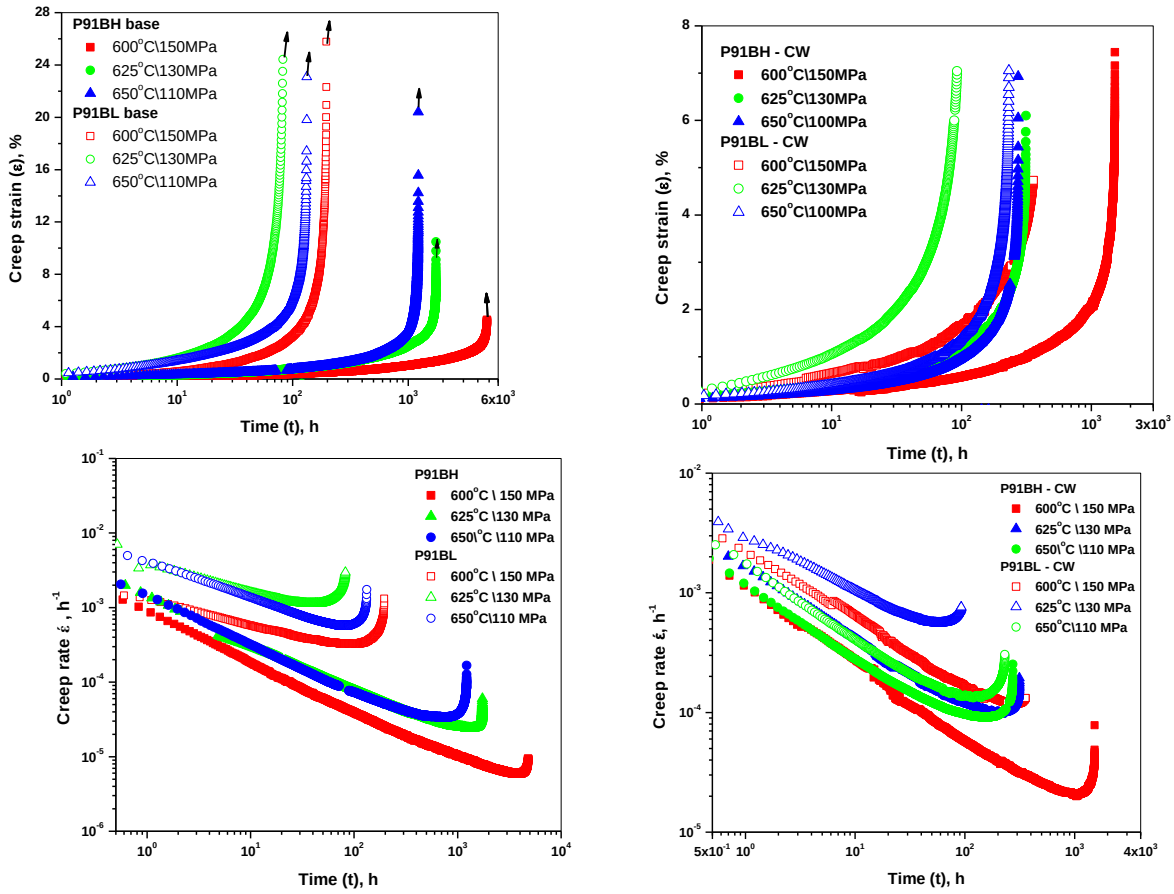

Figure. 3 Typical plots of (a), (b) strain–time ((c), (d) creep rate–time for P91BH and P91BL at test temperatures

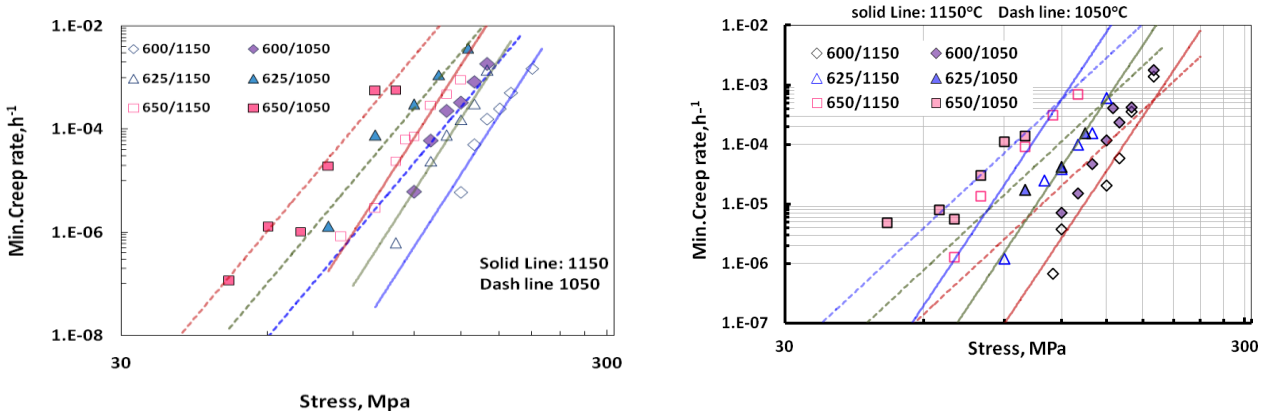

Figure. 4 Stress dependence of minimum creep rate for P91BL and P91BH (a) base metal (b) cross weld specimens

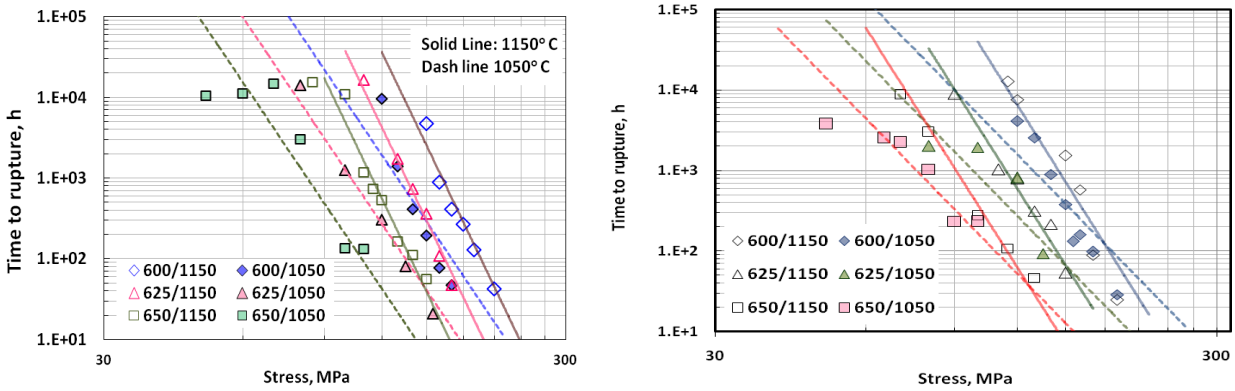

Figure.5 Stress dependence of rupture life for P91BL and P91BH (a) base metal (b) cross weld specimens

Comparative creep behavior of base and weldments for P91BL and P91H revealed higher minimum creep rates (and shorter lives) for weldments than that for the base metal. The extent of decrease in creep life for weldments is found to be higher at longer rupture lives (i.e., at lower stresses). This observation was pronounced at test temperature of 650°C compared to other temperatures. For both base and weldments, minimum creep rates were found to be higher for P91BL than P91BH and in other words, P91BH exhibited longer creep–rupture lives. The observations in the present work are similar to those reported by others for P91 steel [12–14].

3.3. Creep rate and rupture life behavior

Stress dependence of minimum creep rate for base (Figure. 4a) and cross weld specimens (Figure.4b) of P91BL and P91BH obeyed power–law creep equation of the form

$$\dot{\varepsilon}_{\min} = A\sigma^{n} \exp(-Q/RT), \qquad (1)$$

Where A is a constant, n is the power–law creep exponent, T is the temperature in Kelvin and R is the universal gas constant. At a given stress, the variation of minimum creep rate ($\dot{\varepsilon}_{\min}$) with temperature was represented by ln($\dot{\varepsilon}_{\min}$) vs. 1/T plots, where T is in K. The activation energy Q from these plots was obtained as Q = slope × R, where R = 8.314 J mol^{-1}. The values of n and Q are summarized in Table 3, for base and weldments of P91BL and P91BH

Table 3 Value of stress exponents for the P91BH and P91BL steel tested.

Parameter	Material condition			
	P1BH-base	P91BH-Weldment	P91BL-base	P19BL-Weldment
Creep exponent n	14	11	11	7.2
Activation energy (kJ mol^{-1})	651	448	637	427

Observed values of n and Q for the P91BL and P91BH are comparable to that reported [12–14] for P91 steel. It may be noticed from Table 3 that n is higher for P91BH compared to P91BL. Further, n is higher for base metal compared to weldment. Though the observed Q is almost the same for P91BL and P91BH, Q is found to be higher for the base metal than that of the weldment. It may be mentioned that the unrealistically higher values of n and Q have been generally observed for particle/precipitation hardened alloys [16-18]. The detailed analysis incorporating corrections for modulus, diffusivity and resisting stress for dislocation motion (precipitate–dislocation interaction) is required to be performed for rationalizing the higher values of n (than n = 5) and Q (than Q for lattice diffusion in α-iron, Q_l = 250 kJ mol^{-1}). The differences in „n" and Q between the base and weldment may possibly be related to the fine precipitates for base metal compared to coarse precipitates for the weldment. However, it may be suggested that creep behavior of P91B steel is governed by the dislocation climb over precipitates.

Minimum creep rate and rupture life is generally described by the well known Monkman–Grant relationship of the form

$$\dot{\varepsilon}_{\min} t_r = C = C_{MG}, \qquad (2)$$

Where C (i.e., C_{MG} is Monkman–Grant constant). The Monkman–Grant plots for both P91BL and P91BH are shown in Figure.6**.** It was observed that the slope in these plots is nearly equal to unity implying that the Monkman–Grant relationship is valid. The value of constant C is given in the figure for various conditions

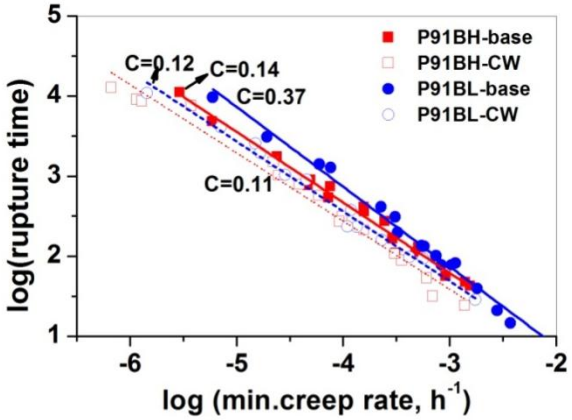

Figure 6 Monkman-Grant relationship for base metal weldments of P91BL and P91BH.

The Monkman–Grant relation is helpful in extrapolation of creep–rupture life at longer durations, knowing the value of minimum creep rate. Extrapolation of long term creep life from

short term tests data can be achieved by the well known Larson–Miller parameter (LMP) which is given as

$$LMP = T(C + \log t_r), \quad (3)$$

Where C is a constant. It has been observed that the value of constant C varies from 20–40. For the results in the present work, C was obtained experimentally that was found to describe the LMP plots adequately. The values of C are given in the LMP plots. For base metal and cross welds of P91BL and P91BH, LMP plots are presented in Figure 7 and Figure 8 for, respectively. Based on Figures. 9 and 10**,** it can be seen that the variation of stress (σ) vs. LMP can be represented as

$$LMP = a_0 + a_1 \log \sigma, \quad (4)$$

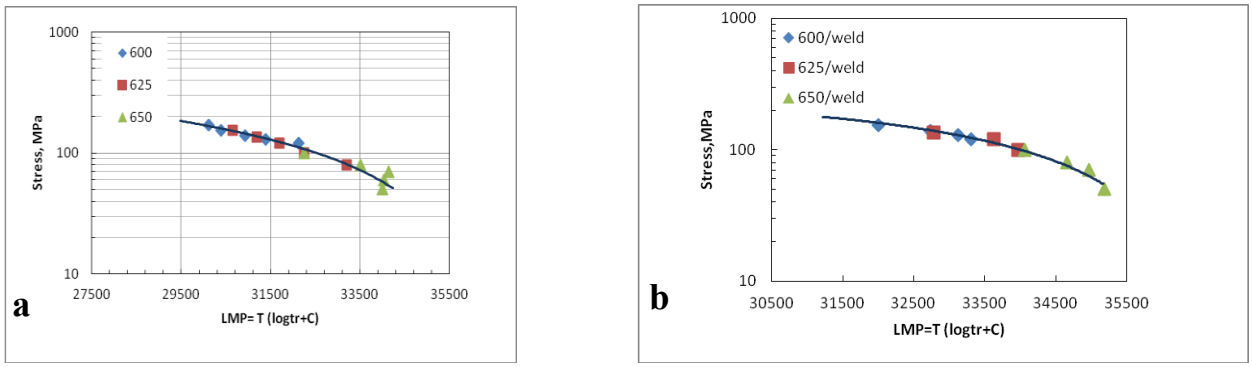

Figure.7. Stress vs. LMP plots for P91BL: (a) base metal and (b) weldment. The value of C = 30 for base metal and C = 23.4 for weldment were obtained based on the regression analysis of test data.

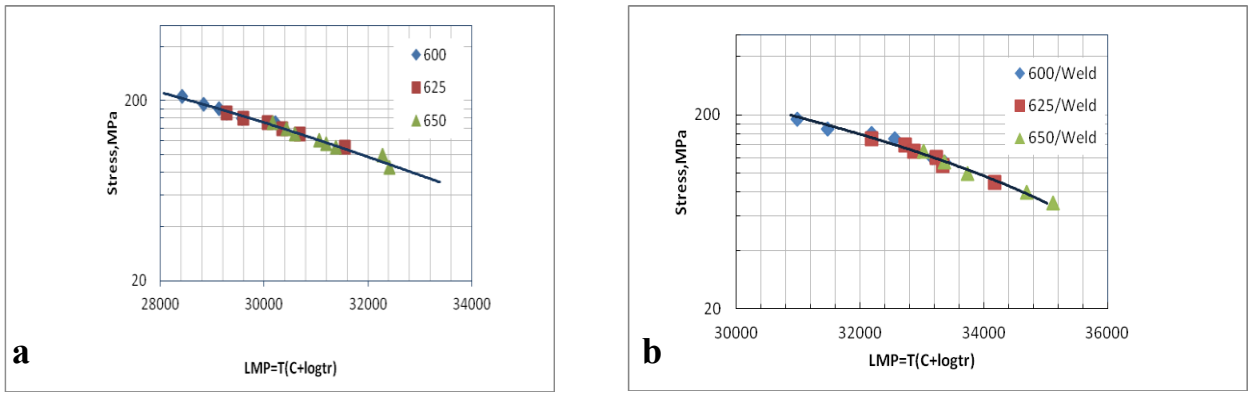

Figure.8. Stress vs. LMP plots for P91BH: (a) base metal and (b) weldment. The value of C = 30 for base metal and C = 34 for weldment were obtained based on the regression analysis of test data.

Where a_0 and a_1 are coefficients. The above equation can be rearranged as the equation of the form given below. This rearranged equation could be employed for evaluating stress values for long–term creep rupture life of 10^5 h and the equation is given as

$$\log t_r = -C + (1/T)(a_0 + a_1 \log \sigma). \quad (5)$$

Knowing a_0, a_1 and C, stress to cause a given t_r (say 10^5 h) could be determined at a specified temperature. In other words one can determine the creep–rupture strength (stress to cause known

t_r) values. The obtained values of stress for 10^5 h of rupture life (i.e., creep–strength) are listed in Table 4. The values got for P91BH base and weldments are better than that for P91BL.

3.4. Weld strength reduction factor

Weldments showed much reduced life compared to the base metal for P91BL and P91BH. This is generally expressed by the weld strength reduction factor. Weld strength reduction factor is given by the ratio of rupture strength of the weldment to that of the base metal. Using Eq. (5), the rupture strength values for 10^5 h can be obtained for both base and weldments for P91BL and P91BH in the temperature range of 600–650°C. The obtained weld strength factors calculated for temperature range 600–650°C are shown in Fig.9. It can be seen that the strength reduction factor is higher for P91BH.

Table 4.Strength values for 10^5 h calculated from experimental data compared with literature values

Temperature	Stress (MPa)						
	P1BH -base	P91BH-weldment	P91 BL-base	P91BL-weldment	P91 base ECCC -2009	P91 base [16]	P91 weldment [16]
600	112	92	79	62	90	91	74
625	93	71	61	45	-	68	53
650	77	56	48	33	48	47	37

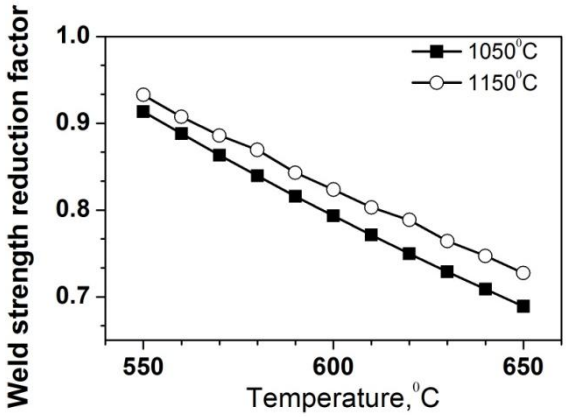

Figure 9. Plot of weld strength reduction factor for P19BL and P91BH at different temperatures.

3.5. Microstructure of P91BH weldments after creep

Similar to that observed for the base metal (Figs. 1 a,b), the cross weld specimens of P91BH also showed the finer precipitates compared to P91BL weldments. This would imply that the microstructure of P91BH weldment is more stable when compared to P91BL weldment. After creep testing, it was observed the precipitates size increased and this increase was pronounced at higher creep test temperatures and at lower stresses for both P91BL and P91BH weldments. Microstructure in the HAZ (for P91BL and P91BH) revealed that the precipitates were found to be coarser in ICHAZ than in the other regions of HAZ. Figure 10 (a,b) shows the SEM image of ICHAZ for P91BH weldment after creep test at 600°C and 130 MPa. Prior austenite grain

boundary and triple point shown as circled is clearly evident in Fig. 10(a). The high magnification image of the circled region is depicted in Fig. 10(b) which clearly reveals the evidence for creep cavitation observed at the precipitate– matrix interface. An important point to make here is that for P91BH weldments, the failure mode was found to shift from Type IV (ICHAZ) to Type II (from weld to HAZ) when the increasing creep test temperature and/or decreasing stress. Whereas for P91BL weldments, the failure was type IV thus illustrating the beneficial role of higher normalizing temperature (i.e., P91BH) in resisting Type IV cracking in P91B steel. This also suggests that the utilization of boron was more effective for P91BH.

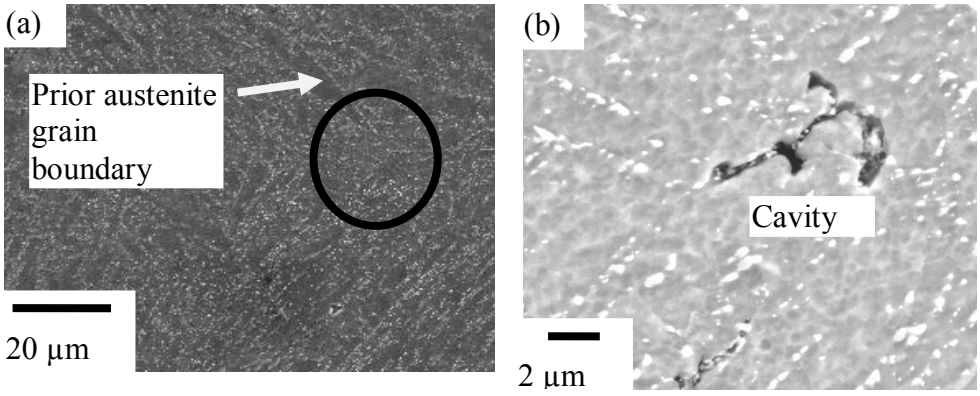

Fig. 10. Microstructure of ICHAZ of P91BH weldment after creep test at 600°C and 130 MPa.

An important point to make here is that for P91BH cross weld specimens, the failure mode was found to shift from Type IV (ICHAZ) to Type II (from weld to HAZ) when the increasing creep test temperature and/or decreasing stress. Whereas for P91BL cross weld specimens, the failure was type IV thus illustrating the beneficial role of higher normalizing temperature (i.e., P91BH) in resisting Type IV cracking in P91B steel. This also suggests that the utilization of boron was more effective for P91BH. Such an observation is seen in Fig. 11. Detail study on crack location is in progress.

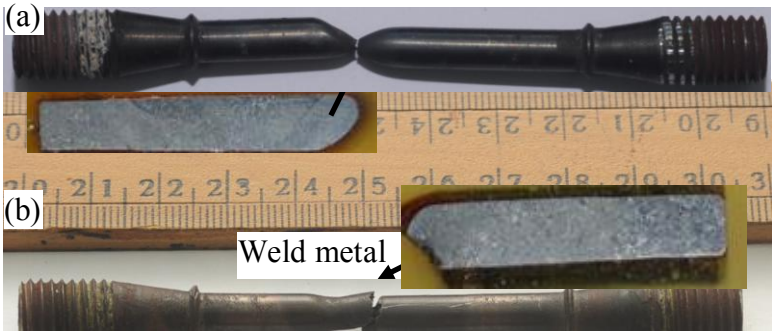

Fig. 11 The photomicrographs of cross weld specimen of (a) P91BL and (b) P91BH creep tested at 600°C and 120 MPa

4. DISCUSSION

Formation and coarsening of subgrains is observed during creep of P91 steel [12–15] which lead to the reduction in dislocation density and it is well known that the subgrain size is inversely related to the stress [5]. Any microstructural changes that resist the dislocation motion and bring

down the growth of subgrains can cause creep rate to decrease. During creep in P91 steel, $M_{23}C_6$ precipitates grow and coarsen. Whereas in P91B, replacement of carbon by boron in $M_{23}C_6$ precipitates during creep reduces coarsening of precipitates [5–7, 15-18]. Hence precipitates observed will be less coarse in P91B steel compared to P91. Finer the precipitate, the stability of microstructure is enhanced. In this study, the finer precipitates observed for P91BH (Figure.1) compared to P91BL can be attributed to the reduction in lath size [8] and increased nucleation sites for precipitation. It has been observed that the prior austenite grain size is higher for P91BH than for P91BL [8,9] and this increase in prior austenite grain size is accompanied by increase in block size [9]. Inverse pole figure maps of P91BL and P91BH base metal show smaller block size for P91BL compared to P91BH (Figure.12 a,b). Block size is observed to be larger for P91BH (7 µm) condition compared to P91BL (4.3 µm) [19] and was measured based on 10° misorientation [9]. The lower creep rates observed for P91BH can be related to the block size, since block size can considered as an effective grain for Ferritic/martensitic steel. This is in line with coarse grain size is preferred for creep at high temperatures

In the P91 cross weld condition, microstructure varies in different regions of HAZ and during creep failure generally occurs in the ICHAZ since this region is prone to creep cavitation damage [5] and strengthening ICHAZ improves creep–rupture life [5,8,9]. For P91B weldments, prior austenite grain size is observed to be almost similar across the HAZ [8] and is closer to that of base metal. In other words, microstructure is more uniform in the weldments of P91B steel as reflected by a smaller difference in the hardness between CGHAZ and ICHAZ implying that the localization of creep strain is less pronounced in P91B steel. This difference in hardness between CGHAZ and ICHAZ gets further reduced for P91BH compared to P91BL condition illustrating the combined beneficial role of boron and higher normalizing temperatures. This is the reason for higher creep– rupture lives and lower minimum creep rates for P91BH as observed in the present study. The higher weld strength factors for P91BH are also related to the uniform and stable microstructure in the HAZ of P91BH weldments

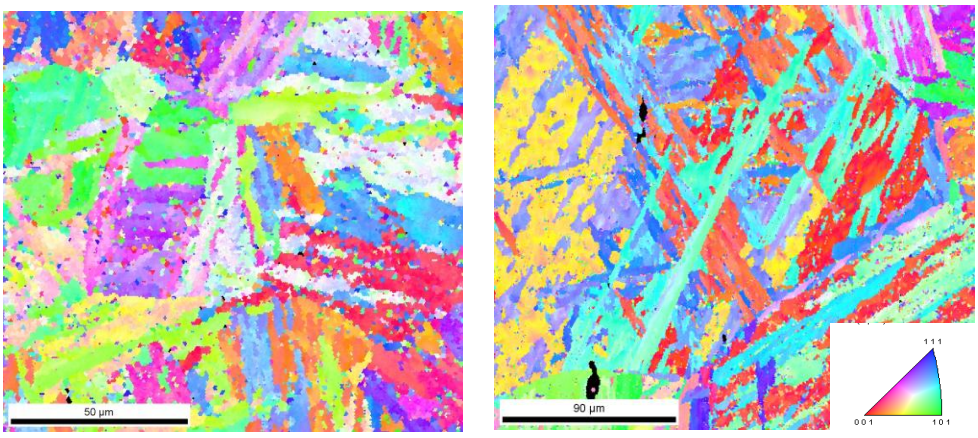

Figure. 12 IPF map obtained from the normalized and tempered (760°C/3h) steels (a) P91BL and (b) P91BH base metal

5. CONCLUSIONS

The following principal conclusions are drawn from this study.
1. P91BH steel showed better creep properties than P91BL in terms of lower minimum creep rate and rupture life for both base metal and weldments.

2. Weld strength reduction factor is found to be higher for P91BH compared to P91BL.
3. Based on the beneficial effect of P91BH steel on creep properties, higher normalizing temperature of 1150°C can be recommended for P91B steels.

REFERENCES

1. Viswanathan R., Gandy D., Coleman K., "*Advances in materials technology for fossil power plants*", (Proc. Conf.) 4th Intnl. Conf. Oct25-28 (2004) EPRI report no. 1011381
2. Santella M., Shingledecker J., *Advanced pressure boundary materials*", 20th Annual conference on Energy materials June 12 (2006), Knoxville, TN.
3. Abe F., "*Creep resistant steels''*, CRC press (2008).
4. Shibli I. A., "Performance of P91 Thick Section Welds Under Steady and Cyclic Loading Conditions: Power Plant and Research Experience", *OMMI* (vol. 1, issue 3 (2002) pp.1–16.
5. Abe F., Tabuchi M., Kondo M., Tsukamoto M., "Suppression of Type IV fracture and improvement of creep strength of 9Crsteel welded joints by boron addition", *Intnl Jl. Pressure Vessels and piping* vol.85 No.(1-2) (2007), pp. 44–51.
6. Semba H., Abe F." Alloy design and creep strength of advanced 9CrUSC boiler steels containing high concentration of boron", *Energy Materials* vol1.No.5/4(2006), pp. 238–244.
7. Tabuchi M., Kondo M., Watanabe T., Hongo H., Yin F., Abe F., "Improvement of Type IV cracking resistance of (Cr heat resisting steel weldment by boron addition", *Acta Metallurgical Sinica* vol.14 No.4 (2004) pp. 331–337.
8. Das C.R., "Improving the creep resistance of modified 9Cr-1Mo steel weldment by microstructural modification", Ph.D. Thesis, 2011 IIT-Madras, India.
9. Das C.R., "Transition of crack from Type IV to Type II resulting from improved utilization of boron in the modified 9Cr-1Mo steel weldment, *Metall. Mater. Trans.* 43A (2012) 3724–3741.
10. Baral J , "Creep behavior of (CrMoVNb(P91) steel containing small amount of boron", M.Tech Thesis, IIT-Kharagpur, India (2011).
11. Das C.R., Albert S. A., Laha K., Swaminathan J, Ravi S., Bhadhuri A.K. and Murty B.S., "Influence of CSL boundary on creep resistance of P91 steel weldments". 1st Int. Conf. on Structural Integrity –ICONS 2014, Feb 4–7, (2014), Kalpakkam, India.
12. Choudhary B K., Issac Samuel., "Creep behavior of modified 9Cr-1Mo ferritic steel", J. of Nuclear. Mater., Vol.412 (2011) pp. 82–89. 13. Triratna Shrestha, Mehdi Basirat, Indrajit Charit, Gabirel P. Potirniche, Karl K Rink and Uttara Sahaym, " Creep deformation mechanism in modified 9Cr1Mo steel", *Jl. of Nuclear Mater.*, vol. 423 (2012) pp. 110–119.
14. Choudhary B K., "Tertiary creep behavior of 9Cr-1Mo ferritic steel", *Mater. Sci. Engg A.*, 585 (2013) pp.1–9.
15. Hald J," Microstructure and long term creep properties of 91-2 Cr steels", *Int. J. Press. Vess. and Piping* 85(2008) pp30–37.
16. D.V.V.Satyanarayana, G. Malakondaiah, D.S.Sarma, *Mater.Sci. Eng.A* 323(2002) 119–128.
17. R.Singh, S.Banerjee, *Acta Metall.Mater*. 40 (1992) 2607 –2616.
18. A.B. Pandey, R.S. Mishra, A.G. Paradkar, Y.R. Mahajan, *Acta Mater.* 45 (1997) 1297–1306
19. Gabriel Potirniche, Indirajit Charit, Karl Rink and Fred Barlow, "Prediction and Monitoring systems for creep -fracture , behavior of 9Cr1Mo steels for reactor pressure vessels", NEUP 2009 project 09-835 (09-458) Final Report, Mechanical Engg. Dept. University of Idaho (2013).
20. Das C.R., Albert S. G. Sasikala A., Bhadhuri A.K. and Murty B.S, *Communicated to Met Trans A*, 2014